THE ASTROPHYSICAL JOURNAL, 599:L17–L20, 2003 December 10

# THE WENDELSTEIN CALAR ALTO PIXELLENSING PROJECT[1] (WeCAPP): FIRST MACHO CANDIDATES

ARNO RIFFESER, JÜRGEN FLIRI, RALF BENDER, STELLA SEITZ, AND CLAUS A. GÖSSL
Universitäts-Sternwarte München, Scheinerstrasse 1, D-81679 München, Germany; arri@usm.uni-muenchen.de
*Received 2003 January 8; accepted 2003 October 28; published 2003 November 20*

## ABSTRACT

We report the detection of the first two microlensing candidates from the Wendelstein Calar Alto Pixellensing Project (WeCAPP). Both are detected with a high signal-to-noise ratio and were filtered out from 4.5 million pixel light curves using a variety of selection criteria. Here we only consider well-sampled events with timescales of 1 day $< t_{\rm fwhm} <$ 20 days, high amplitudes, and a low $\chi^2$ of the microlensing fit. The two-color photometry $(R, I)$ shows that the events are achromatic and that giant stars with colors of $(R-I) \approx 1.1$ mag in the bulge of M31 have been lensed. The magnification factors are 64 and 10, which are obtained for typical giant luminosities of $M_I = -2.5$ mag. Both lensing events lasted for only a few days ($t^{\rm GL1}_{\rm fwhm} = 1.7$ days and $t^{\rm GL2}_{\rm fwhm} = 5.4$ days). The event GL1 is likely identical with PA-00-S3 reported by the POINT-AGAPE project. Our calculations favor in both cases the possibility that MACHOs in the halo of M31 caused the lensing events. The most probable masses, 0.08 $M_\odot$ for GL1 and 0.02 $M_\odot$ for GL2, are in the range of the brown dwarf limit of hydrogen burning. Solar mass objects are a factor of 2 less likely.

*Subject headings:* dark matter — galaxies: halos — galaxies: individual (M31) — Galaxy: halo — gravitational lensing

## 1. INTRODUCTION

Microlensing experiments are an ideal method to search for dark objects within and between galaxies. A large number of microlensing events have been detected toward the Galactic bulge, constraining the number density of faint stars in this direction (Alard 1999; Derue et al. 1999; Alcock et al. 2000b; Udalski et al. 2000). Toward the LMC, only 13–17 microlensing events have been reported so far (Alcock et al. 2000a). If all these events are attributed to 0.5 $M_\odot$ MACHOs, the associated population of dark objects would contribute up to the 20% level to the dark matter content of the Milky Way (Alcock et al. 2000a). However, both the relatively large size of the LMC relative to its distance and the nature of the lenses have cast doubt on this interpretation. It is indeed likely that a large fraction of the microlensing events toward the LMC are due to self-lensing of stars within the LMC (see Lasserre et al. 2000, Evans & Kerins 2000, and references therein).

Studying microlensing events toward M31 allows us to separate self-lensing and halo lensing in a statistical way since the optical depth for halo lensing is larger on the far side of M31. In M31, individual stars cannot be resolved, and one therefore has to use the pixellensing technique (Crotts 1992; Baillon et al. 1993) to follow the variability of sources blended with thousands of other sources within the same pixel. First detections of possible microlensing events were reported by several pixellensing experiments (Crotts & Tomaney 1996; Ansari et al. 1999; Aurière et al. 2001; Paulin-Henriksson et al. 2002, 2003; Calchi Novati et al. 2003). But since the candidate nature of only five of these events is convincing, no conclusions concerning the near-far asymmetry or the most likely dark matter lensing masses could be drawn yet.

The Wendelstein Calar Alto Pixellensing Project (WeCAPP; Riffeser et al. 2001) started in 1997 with test observations. Since 1999, the bulge of M31 was monitored continuously during the time of visibility of M31. The analysis of our 4 yr data will allow not only the identification of very short duration events (e.g., in the fourth year, data of the combined field have been taken on 83% of possible nights) but also the separation of long-duration microlensing events from long periodic variables like Mira stars. For this Letter, we analyzed the short-duration events ($t_{\rm fwhm} <$ 20 days) within one season of Calar Alto data and restricted the detection to high signal-to-noise ratio (S/N), high-magnification events. We report our first two microlensing candidates of that type.

## 2. OBSERVATIONS AND DATA REDUCTION

WeCAPP monitors the central region of M31 in a 17.2 × 17.2 arcmin$^2$ field with the 1.23 m telescope of the Calar Alto Observatory. In addition, a quarter of this field, pointing toward the far side of the M31 disk along the southeast minor axis, was observed with the 0.8 m telescope of the Wendelstein Observatory. The data analysis and candidate selection reported in this Letter are based on the season from 2000 June 23 to 2001 February 25 and are restricted to the Calar Alto data only. During this period, M31 was observed during 43% of all nights. Observations were carried out in $R$ and $I$ filters close to the Kron-Cousins system. We estimate the systematic error in the $(R-I)$ color to be $\leq 0.05$ mag.

We have developed a pipeline based on the work of Gössl & Riffeser (2002) and A. Riffeser, J. Fliri, & C. A. Gössl (2004, in preparation) that performs the standard CCD reduction, position alignment, photometric alignment, stacking of frames, matching of the point-spread function (PSF) using optical image subtraction (Alard & Lupton 1998), and the generation of difference images. For the data presented here, all data within one night are co-added, yielding one difference image per night. The reduction package includes full error propagation for each pixel through all reduction steps. In this way, all data points are properly taken into account in the search for variables.

---

[1] Based on observations at the Wendelstein Observatory of the University Observatory Munich and at the German-Spanish Astronomical Center, Calar Alto, operated jointly by the Max-Planck-Institut für Astronomie, Heidelberg, and the Spanish National Commission for Astronomy.

TABLE 1
Selection Criteria

| Criterion | Number |
|---|---|
| Analyzed light curves | 4492250 |
| Light curves with >10 data points | 3835407 |
| Three successive 3 $\sigma$ in $R$ or $I$ | 517052 |
| $\chi^2_R < 1.3$ and $\chi^2_I < 1.3$ | 186039 |
| 1 day < $t_{\rm fwhm}$ < 20 days | 9497 |
| 3 $\sigma$ light point inside $t_{\rm fwhm}$ | 1829 |
| Sampling: side$_1$ > 20%, side$_2$ > 5% | 256 |
| $F_{\rm eff} > 10$ median$_{\rm error}$ in $R$ and $I$ | 15 |
| Candidates | 2 |

## 3. SELECTION CRITERIA

We investigate only pixels that have more than 10 data points in $R$ and $I$, which applies to 85% of the 2K × 2K field. For each pixel, we define a flux baseline by the iterative 3 $\sigma$ clipping of all outliers with higher flux. All pixels that have at least three successive (positive) 3 $\sigma$ deviations from this baseline are considered as variables. We fitted the microlensing light curve for high-amplification events (Gould 1996) simultaneously to the $R$- and $I$-band pixel light curves for every variable. The fit has six free parameters: the full width at half-maximum $t_{\rm fwhm}$ and the time $t_0$ of maximum amplification (these two parameters are the same for both filters), amplitude $F_{{\rm eff},\,R}$, color $F_{{\rm eff},\,I}/F_{{\rm eff},\,R}$, and baseline levels $c_R$ and $c_I$. Variables with a reduced $\chi^2_R > 1.3$ or $\chi^2_I > 1.3$ are discarded. In this way, we exclude light curves that are not achromatic or that are not symmetric. We also exclude events with $t_{\rm fwhm} > 20$ days, which can be confused with long periodic variables like Mira stars, as long as only one season of data is investigated. In addition, all candidates that do not have at least one significant data point (3 $\sigma$ deviation from the baseline) within $t_{\rm fwhm}$ of the time of maximum amplification are rejected. We further define the sampling quality for the falling and rising parts of each light curve within $(t_0 - 15 \text{ days}, t_0)$ and $(t_0, t_0 + 15 \text{ days})$; within these time intervals, we require a sampling of the area under the light curve of at least 20% on one side and of at least 5% on the other side (Table 1).

Here, we only present the two microlensing candidates that have amplitudes 10 times larger than the median error of the light curve (see Fig. 1). Both candidates fit perfectly with a symmetric microlensing light curve. Ruling out systematic offsets for the points and errors on the trailing side of GL2 (which is strongly proved by the six single images of that night in each filter), a nonmicrolensing light curve of a variable source hardly fits the data points of GL2. Both microlensing candidates are detected in several pixels (11 for GL1 and 4 for GL2) inside the PSF of the position of the lensed object. This explains the reduction from 15 events to two events in the last line of Table 1. The amplification light curves were obtained by calculating the total flux within the PSF area of each microlensing event.

For both candidates, the selection criteria exclude variable stars like Miras, novae, or dwarf novae. Extracting lensing events with less good time sampling or lower amplitude or events located close to other variables requires refined selection criteria. These will be discussed in a future paper that will also include a test of the detection efficiency and false detection rate with Monte Carlo simulations.

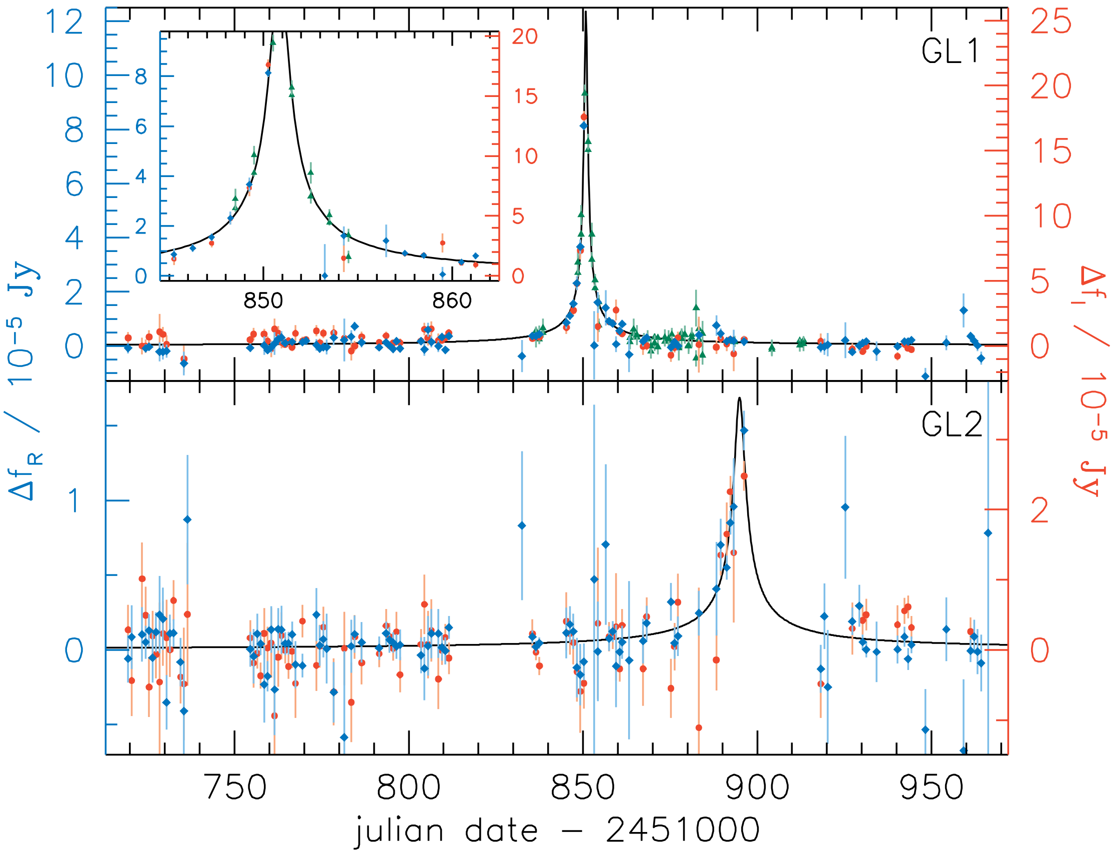

Fig. 1.—Light curves of WeCAPP-GL1 and WeCAPP-GL2. The $I$-band light curve (*red symbols, right axis*) has been scaled to the $R$-band light curve (*blue symbols, left axis*). The scaling factors were derived from the lensing fit (*black curve*) and correspond to a color ($R-I$) of 1.05 for GL1 and 1.08 for GL2. In addition, we show the $r'$ and $i'$ data from the POINT-AGAPE PA-00-S3 event (*green symbols*) scaled to our data.

## 4. MICROLENSING CANDIDATES

The parameters of both lensing candidates are summarized in Table 2. Their light curves are shown in Figure 1. GL1, the highest S/N lensing event candidate in our sample, lies $4'.1$ to the southwest of the nucleus of M31. GL2 is $4'.4$ to the northwest of the nucleus. Our data have been astrometrically calibrated using bright foreground stars observed with the *Hubble Space Telescope* by Jablonka et al. (1999) and with ground-based observations by Magnier et al. (1992). Our two calibrations agree within $0''.5$ in declination and $0''.7$ in right ascension, consistent with the astrometric accuracy of $0''.8$–$1''.0$ of the Magnier et al. catalog. After we had detected GL1 and GL2, we cross-checked with events reported by the POINT-AGAPE survey for the same period of time and the same field in M31 (Paulin-Henriksson et al. 2003). It appears that GL1 is likely identical with PA-00-S3, which occurred at the same time (Fig. 1). Because POINT-AGAPE did not provide a flux calibration of their data, we had to assume a scaling factor for the amplitude. The zero point in time was not adjusted. The data points from WeCAPP and POINT-AGAPE complement each other nicely and make GL1 the best pixellensing event found so far in M31. GL2 also falls in the observing period covered by POINT-AGAPE, but their time sampling around the event is poor. This may be the reason why GL2 was not detected.

The parameters of the lensing fit are degenerate for high magnifications (Gould 1996), i.e., for amplitudes $A_0 \gg 1$ that correspond to impact angles much smaller than the Einstein angle $\theta_{\mathrm{E}}$. In this case, for the light curve, we obtain $F_0[A(t) - 1] \rightarrow F_{\mathrm{eff}}[(12/t_{\mathrm{fwhm}}^2)\,(t - t_0)^2 + 1]^{-1/2}$, with $F_0$ being the intrinsic flux of the source and $F_{\mathrm{eff}} = F_0/u_0 \approx F_0 A_0$, where $u_0$ is the impact angle in units of the Einstein angle.

In order to obtain $A_0$, we evidently need to know the source flux $F_0$. We can get rough constraints by considering the colors of the light curves, which, due to our selection criteria, are achromatic. We obtain $(R-I)_{\mathrm{GL1}} = 1.05$ and $(R-I)_{\mathrm{GL2}} = 1.08$. For main-sequence stars, this converts[2] (Cassisi et al. 1998) into absolute magnitudes of $M_I \approx 8$ mag. If the sources are giants, then the magnitudes are $M_I = -2.5$ mag with a minimum of $-1.9$ and a maximum of $-3.7$ (Bessell 1979; Grillmair et al. 1996). We now derive the lensing parameters as follows: $u_0 = F_{0,\,I}/F_{\mathrm{eff},\,I} \rightarrow t_{\mathrm{E}} = t_{\mathrm{fwhm}}/(u_0\sqrt{12}) \rightarrow M_{\mathrm{lens}} = (v_t t_E)^2 c^2 D_S/\,[4GD_L(D_S - D_L)]$, where $t_{\mathrm{E}}$ is the Einstein timescale, $v_t$ is the transverse velocity between source and lens, and $D_L$ and $D_S$ are the angular distances to the lens and source, respectively.

To estimate plausible lens masses, the Einstein timescales $t_{\mathrm{E}}$ are calculated for fixed luminosities of possible source stars (see Table 2). Note that the errors in $t_{\mathrm{E}}$ reflect the accuracy of the determination of $t_{\mathrm{fwhm}}$ in the degenerate Gould fit only and do not account for the systematic uncertainties due to the unknown luminosities of the sources. If the source is a main-sequence star, we need very high magnifications, $A_0 \approx 10^5$–$10^6$. The corresponding lens masses (for $v_t = 210$ km s$^{-1}$, $D_L = 768$ kpc, $D_S = 770$ kpc) are $M \approx 10^7$–$10^8\ M_\odot$, an implausibly large value. If the source is a giant, the required magnifications are reduced to $A_{0,\,\mathrm{GL1}} = 64$ and $A_{0,\,\mathrm{GL2}} = 10$; the typical self-lensing masses become $M = 0.8\ M_\odot$ and $M = 0.2\ M_\odot$.

TABLE 2

Parameters of the Microlensing Candidates

| Parameter | GL1 | GL1, PA-00-S3[a] | GL2 |
|---|---|---|---|
| $\alpha_{\mathrm{J2000}}$ | $00^{\mathrm{h}}42^{\mathrm{m}}30^{\mathrm{s}}.3$ | $00^{\mathrm{h}}42^{\mathrm{m}}30^{\mathrm{s}}.3$ | $00^{\mathrm{h}}42^{\mathrm{m}}32^{\mathrm{s}}.8$ |
| $\delta_{\mathrm{J2000}}$ | $+41^\circ13'00''.8$ | $+41^\circ13'00''.8$ | $+41^\circ19'56''.5$ |
| $t_0$ (JD$-$2,451,000) | 850.80 ± 0.13 | 850.84 ± 0.02 | 894.77 ± 0.21 |
| $t_{\mathrm{fwhm}}$ (days) | 1.38 ± 0.53 | 1.65 ± 0.10 | 5.41 ± 2.49 |
| $F_{\mathrm{eff},\,R}$ ($10^{-5}$ Jy) | 13.4 ± 5.4 | 12.4 ± 0.6 | 1.7 ± 0.5 |
| $F_{\mathrm{eff},\,I}$ ($10^{-5}$ Jy) | 28.0 ± 11.2 | 25.7 ± 1.5 | 3.6 ± 1.1 |
| $(R-I)$[b] | 1.05 ± 0.08 | 1.05 ± 0.08 | 1.08 ± 0.24 |
| $\chi^2$ | 1.23 | 1.22 | 1.02 |
| $M_I = -1.9$ mag | | | |
| $A_0$ | 120 | 110 | 16 |
| $t_{\mathrm{E}}$ (days) | 47.4 ± 18.1 | 52.1 ± 3.2 | 23.9 ± 11.0 |
| $M_I = -2.5$ mag | | | |
| $A_0$ | 69 | 64 | 10 |
| $t_{\mathrm{E}}$ (days) | 27.2 ± 10.4 | 30.0 ± 1.8 | 13.8 ± 6.3 |
| $M_I = -3.7$ mag | | | |
| $A_0$ | 24 | 22 | 4 |
| $t_{\mathrm{E}}$ (days) | 9.0 ± 3.5 | 9.9 ± 0.6 | 4.6 ± 2.1 |
| $M_I = 7.7$ mag | | | |
| $A_0$ | $8.2 \times 10^5$ | $7.6 \times 10^5$ | $1.1 \times 10^5$ |
| $t_{\mathrm{E}}$ ($10^5$ days) | 3.3 ± 1.3 | 3.6 ± 0.2 | 1.7 ± 0.8 |

[a] Derived from a fit to the total set of data points (WeCAPP and POINT-AGAPE).

[b] The systematic error in the $(R-I)$ color is ≤0.05 mag.

Assuming the source to be a red giant with $M_I = -2.5$ mag, we calculate the probability $p(M, t_{\mathrm{E}})$ that a microlensing event of an observed timescale $t_{\mathrm{E}}$ can be produced by a lens of the mass $M$. Following the calculations of Jetzer & Massó (1994; eq. [8]) and Jetzer (1994; eq. [11]), we get

$$p(M, t_{\mathrm{E}}) \sim \xi(M) \int \rho_S(D_S) \int \rho_L(D_L)\, f\left(\frac{R_{\mathrm{E}}}{t_{\mathrm{E}}}\right) \frac{R_{\mathrm{E}}^3}{t_{\mathrm{E}}^3}\ dD_L\, dD_S,$$

where $\xi(M)$ is the mass function (MF), $\rho_s(D_S)$ is the sources' density, $\rho_l(D_L)$ is the lenses' density, $f(v_t)$ is the velocity distribution, and $R_{\mathrm{E}}(D_L, M, D_S)$ is the Einstein radius.

The distribution of matter in the central part of M31 is based on the bulge model of Kent (1989). The disk is modeled with a radial scale length of 6.4 kpc and an exponential shape and with a vertical scale length of 0.3 kpc and a sech$^2$ shape. The halo is modeled as an isothermal sphere with a core radius of $r_c = 2$ kpc. The velocity distribution was calculated from a Maxwellian halo bulge and disk velocity distribution with an additional rotation for bulge and disk (Kerins et al. 2001).

For the bulge lenses, we take the MF as derived for the galactic bulge, $\xi \sim M^{-1.33}$ (Zoccali et al. 2000). For the disk population, we adopt a Gould MF $\xi \sim M^{-2.21}$ with a flattening $\xi \sim M^{-0.56}$ below 0.59 $M_\odot$ (Gould, Bahcall & Flynn 1997). Both are cut at the lower end at the hydrogen-burning limit of 0.08 $M_\odot$. At the upper end, the bulge MF is cut at the main-sequence turnoff of 0.95 $M_\odot$ (C. Maraston 2003, private communication), and the disk MF is cut at 10 $M_\odot$. The MF for the potential MACHO population residing in the halo of M31 is of course unknown. We therefore calculate the probability distribution for halos consisting of one mass only, i.e., taking $\delta$-function MFs centered on the lens mass $\xi = \delta(M - M_{\mathrm{lens}})/M_{\mathrm{lens}}$. Moreover, we assume that the whole dark halo of M31 consists of MACHOs. Lensing by Galactic halo objects has an order-of-magnitude smaller optical depth and is therefore neglected in our considerations.

The results are shown in Figure 2. For M31 halo lenses, the most probable masses are 0.08 $M_\odot$ for GL1 and 0.02 $M_\odot$ for GL2. In the case of self-lensing, the most probable masses are

---

[2] Transformed on the observational plane by Maraston (1998).

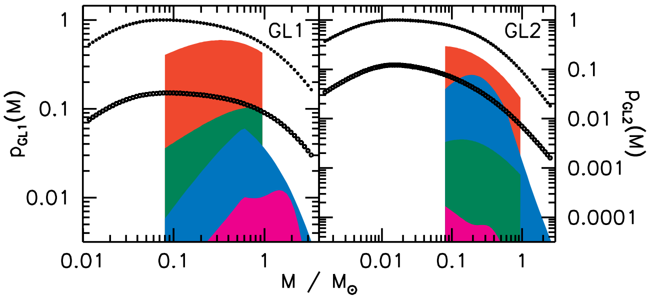

FIG. 2.—Mass probability for GL1 (*left panel*) and GL2 (*right panel*) for lens-source configurations: halo-bulge (*filled circles*), halo-disk (*open circles*), bulge-bulge (*red*), bulge-disk (*green*), disk-bulge (*blue*), and disk-disk (*magenta*). The maximum of each curve is scaled to reflect the total probability of a respective lens-source event relative to the case of a halo-bulge lensing event with the most probable MACHO mass. For example, in the case of GL1, the probability for bulge-bulge lensing relative to halo-bulge lensing with 0.08 $M_\odot$ lenses becomes 0.6 (maximum of red curve). A halo consisting of 0.014 $M_\odot$ MACHOs would have the same probability as bulge-bulge lensing. Note that the shapes of the distributions for bulge and disk lenses are strongly affected by the mass function $\xi(M)$ used.

about a factor of 4 bigger. Taking the most likely halo lens masses, the ratio of the probabilities that the lenses are part of the dark halo or the stellar content $p_{\rm halo}/(p_{\rm bulge} + p_{\rm disk})$ is 1.6 for GL1 and 3.3 for GL2. We conclude therefore that it is likely that lenses residing in the halo of M31 caused the events in both cases.

## 5. DISCUSSION AND OUTLOOK

We presented the first two high (S/N), short-timescale microlensing events from WeCAPP. GL1 is likely identical to PA-00-S3 found by POINT-AGAPE. Combining the data from AGAPE with ours shows that the error bar of the derived Einstein timescale becomes smaller by a factor of 5 compared with the individual error bar. This demonstrates the importance of a good time sampling of the events. We derived the colors of the lensed stars, the amplification factors, and the likely lens masses for both bulge/disk self-lensing and halo lensing. We showed that red giants are the likely source objects, while main-sequence stars are highly implausible.

Self-lensing in the bulge can only be separated from halo lensing statistically. Halo lensing events show a spatial asymmetry because the optical depth for lensing events is higher for stars on the far side of M31 than for stars on the near side (Crotts 1992; J. Fliri et al. 2004, in preparation). In contrast, bulge self-lensing is symmetric.

The bulge self-lensing hypothesis yields lensing stars at or below the main-sequence turnoff of the M31 bulge. On the other hand, if the lensing events are caused by MACHOs, their masses are typically very low, most probable below 0.1 $M_\odot$. Masses in the range of 0.5–1 $M_\odot$ are more unlikely.

So far, we have analyzed one observing season and restricted the lensing search to short-time, high-amplification events in order to avoid confusion with variable stars. The whole WeCAPP data set will allow us to identify all variables and thus will enable us to search for lower amplitude and longer duration microlensing events.

Decreasing the amplitude threshold will increase the detected rate of events in two ways. As the event rate is proportional to the inverse of the minimum required magnification $A_{0,\,\rm min}$ in the pixellensing regime, we expect to detect more lensed giants. On the other hand, lowering the amplification threshold could also make it possible to detect highly amplified main-sequence stars (Han & Gould 1996) that exceed the evolved stars in the bulge of M31 by a factor of more than a hundred. How many more lensing events will be detected depends on the mass function of the lenses, but we can expect at least a factor of a few (J. Fliri et al. 2004, in preparation).

Finally, the effects of time sampling and of the noise properties of our sample on the detectability of lensing events have to be taken into account. The results of the modeling of these effects for events of different durations and amplitudes using Monte Carlo simulations will be presented in a future publication. With the full data set, we expect to increase the number of lensing events in order to detect the predicted asymmetry of MACHO lensing or to rule out a significant MACHO population in the halo of M31.

This work was supported by the *SFB 375 Astro-Particle-Physics* of the Deutsche Forschungsgemeinschaft.

## REFERENCES

Alard, C. 1999, A&A, 343, 10
Alard, C., & Lupton, R. H. 1998, ApJ, 503, 325
Alcock, C., et al. 2000a, ApJ, 542, 281
———. 2000b, ApJ, 541, 734
Ansari, R., et al. 1999, A&A, 344, L49
Aurière, M., et al. 2001, ApJ, 553, L137
Baillon, P., Bouquet, A., Giraud-Heraud, Y., & Kaplan, J. 1993, A&A, 277, 1
Bessell, M. S. 1979, PASP, 91, 589
Calchi Novati, S., Jetzer, Ph., Scarpetta, G., Giraud-Héraud, Y., Kaplan, J., Paulin-Henriksson, S., & Gould, A. 2003, A&A, 405, 851
Cassisi, S., Castellani, V., degl'Innocenti, S., & Weiss, A. 1998, A&AS, 129, 267
Crotts, A. P. S. 1992, ApJ, 399, L43
Crotts, A. P. S., & Tomaney, A. B. 1996, ApJ, 473, L87
Derue, F., et al. 1999, A&A, 351, 87
Evans, N. W., & Kerins, E. 2000, ApJ, 529, 917
Gössl, C. A., & Riffeser, A. 2002, A&A, 381, 1095
Gould, A. 1996, ApJ, 470, 201
Gould, A., Bahcall, J., & Flynn, C. 1997, ApJ, 482, 913
Grillmair, C. J., et al. 1996, AJ, 112, 1975
Han, C., & Gould, A. 1996, ApJ, 473, 230
Jablonka, P., Bridges, T. J., Sarajedini, A., Meylan, G., Maeder, A., & Meynet, G. 1999, ApJ, 518, 627
Jetzer, Ph. 1994, ApJ, 432, L43
Jetzer, Ph., & Massó, E. 1994, Phys. Lett. B, 323, 347
Kent, S. 1989, AJ, 97, 1614
Kerins, E., et al. 2001, MNRAS, 323, 13
Lasserre, T., et al. 2000, A&A, 355, L39
Magnier, E. A., Lewin, W. H. G., van Paradijs, J., Hasinger, G., Jain, A., Pietsch, W., & Trümper, J. 1992, A&AS, 96, 379
Maraston, C. 1998, MNRAS, 300, 872
Paulin-Henriksson, S., et al. 2002, ApJ, 576, L121
———. 2003, A&A, 405, 15
Riffeser, A., et al. 2001, A&A, 379, 362
Udalski, A., Żebrun, K., Szymański, M., Kubiak, M., Pietrzyński, G., Soszyński, I., & Woźniak, P. 2000, Acta Astron., 50, 1
Zoccali, M., Cassisi, S., Frogel, J. A., Gould, A., Ortolani, S., Renzini, A., Rich, R. M., & Stephens, A. W. 2000, ApJ, 530, 418